# HSPA8 inhibitors augment cancer chemotherapeutic effectiveness via potentiating necroptosis

Erpeng Wu[a,b,*], Chenlu Wu[a], Kelong Jia[a], Shen'ao Zhou[c], and Liming Sun[a,*,#]

[a]Shanghai Institute of Biochemistry and Cell Biology, Center for Excellence in Molecular Cell Science, Chinese Academy of Sciences, University of Chinese Academy of Sciences, Shanghai 200031, China; [b]Department of Respiratory Medicine, Shanghai Chest Hospital, Shanghai Jiao Tong University School of Medicine, Shanghai 200030, China; [c]Celliver Biotechnology Inc., Shanghai 200030, China

**ABSTRACT** **Our recent work has uncovered a novel function of HSPA8 as an amyloidase, capable of dismantling the RHIM-containing protein fibrils to suppress necroptosis. However, the impact of HSPA8 inhibitors on cancer regression via necroptosis remains unexplored. In this study, we conducted a comprehensive investigation to assess the potential of HSPA8 inhibitors in enhancing necroptosis both in vitro and in vivo. Our findings indicate that pharmacologic inhibition of HSPA8, achieved either through VER (VER-155008) targeting the nucleotide binding domain or pifithrin-μ targeting the substrate binding domain of HSPA8, significantly potentiates necroptosis induced by diverse treatments in cellular assays. These inhibitors effectively disrupt the binding of HSPA8 to the RHIM protein, impeding its regulatory function on RHIM amyloid formation. Importantly, HSPA8 inhibitors significantly enhanced cancer cell sensitivity to microtubule-targeting agents (MTAs) in vitro, while reversing chemoresistance and facilitating tumor regression by augmenting necroptosis in vivo. Our findings suggest a promising therapeutic approach to cancer through necroptosis modulation via HSPA8 targeting, particularly in combination with MTA drugs for enhanced treatment efficacy.**

## SIGNIFICANCE STATEMENT

- Background: RHIM-amyloids are required for necroptosis. HSPA8, a recently discovered amyloidase, dismantles these fibrils to suppress necroptosis. How pharmacological inhibition of HSPA8 contributes to chemo-induced cancer cell necroptosis is unknown.
- Key Results: This study demonstrates that pharmacologic inhibitors targeting HSPA8 significantly enhance necroptosis in cancer cells. By blocking HSPA8's activity, these inhibitors potentiate the effects of cancer treatments, reversing chemoresistance and promoting tumor regression.
- Implications: Targeting HSPA8 through pharmacologic inhibitors offers a promising therapeutic strategy for cancer treatment. This approach could be particularly effective in combination with MTAs, leading to enhanced treatment efficacy.

**Monitoring Editor**
Guangshuo Ou
Tsinghua University

Received: Apr 30, 2024
Revised: Jun 17, 2024
Accepted: Jun 24, 2024

This article was published online ahead of print in MBoC in Press (http://www.molbiolcell.org/cgi/doi/10.1091/mbc.E24-04-0194) on July 11, 2024.

Author contributions: L.S. and E.W. conceived and designed the experiments; L.S., E.W., K.J., C.W., and S.Z. analyzed the data; L.S. and E.W. drafted the article; L.S. and E.W. prepared the digital images; E.W., K.J., C.W., and S.Z. performed the experiments.

[#]Lead Corresponding Author: Liming Sun, Ph.D.

*Address correspondence to: Erpeng Wu (wuerpeng6@sibcb.ac.cn); Liming Sun (liming.sun@sibcb.ac.cn).

Abbreviations used: DAI, DNA dependent activator of interferon regulatory factors; MTAs, microtubule-targeting agents; NBD, nucleotide binding domain; RHIM, RIP homotypic interaction motif; RIP1, receptor-interacting serine/threonine-protein kinase 1; RIP3, receptor-interacting serine/threonine-protein kinase 3; SBD, substrate binding domain; TRIF, TIR-domain-containing adapter-inducing interferon-β.

## INTRODUCTION

Cancer, a fatal disease marked by the unchecked multiplication of abnormal cells and their dissemination throughout the body, remains a leading cause of mortality worldwide (2023). Traditional cancer chemotherapy regimens primarily rely on apoptosis, an immune-silent mode of cell death triggered by therapeutic agents. However, due to the intratumor heterogeneity and tumor evolution, many cancers develop resistance to apoptosis, particularly among patients who have undergone multiple cycles of chemotherapy (Fanale *et al.*, 2017). In the face of this apoptosis resistance, necroptosis has emerged as a crucial complementary treatment strategy. Necroptosis offers a promising approach to cancer therapy by combining cellular suicide with the immune response, thereby enhancing the anticancer response of organisms (Meier *et al.*, 2024). Unlocking necroptosis in cancer cells is a key research focus, as leveraging this process could yield more effective cancer treatments.

Necroptosis, a form of inflammatory cell death, is triggered by a diverse array of receptors, including TNFR1 embedded in cell membranes, as well as pathogen recognition receptors such as TLR3/4 and Z-DNA sensors like DAI (Sun and Wang, 2014; Pasparakis and Vandenabeele, 2015; Dondelinger *et al.*, 2016; Vanden Berghe *et al.*, 2016; Grootjans *et al.*, 2017; Ai *et al.*, 2024; Yuan and Ofengeim, 2024). These receptors trigger necroptosis by activating RIP3 (receptor-interacting protein kinase 3) through RHIM–RHIM interactions with upstream proteins that have RHIM domains, such as RIP1, DAI, and TRIF. These proteins integrate different signals of cell death from the upstream pathways (He *et al.*, 2011; Upton *et al.*, 2012; Morgan and Kim 2022; Tummers and Green 2022). Once RIP3 is activated, it undergoes autophosphorylation and subsequently activates its substrate MLKL (mixed lineage kinase domain-like protein) (Sun *et al.*, 2012). The activated MLKL oligomerizes and translocates to the cytomembrane, ultimately leading to membrane rupture and necroptosis (Cai *et al.*, 2014; Chen *et al.*, 2014; Dondelinger *et al.*, 2014; Hildebrand *et al.*, 2014; Wang *et al.*, 2014).

Importantly, the RHIM proteins (the RHIM domain-containing proteins) form functional amyloid fibrils, which are crucial for the necroptosis signaling transduction (Li *et al.*, 2012; Sun, 2023). Through RHIM–RHIM interactions, the initiator RHIM proteins (RIP1, TRIF, and ZBP1) recruit the effector RHIM protein RIP3 to form hetero-RHIM fibrils, which serve as seeds for RIP3's further self-assembly into homo-RHIM fibrils. This process promotes RIP3 kinase activity and subsequently recruits its substrate MLKL (Wu *et al.*, 2014; Mompeán *et al.*, 2018; Pham *et al.*, 2019, Hu *et al.*, 2021; Wu, Ma *et al.*, 2021; Wu, Hu *et al.*, 2021; Baker *et al.*, 2022; Chen *et al.*, 2022). The viral RHIM proteins, specifically M45 encoded by murine cytomegalovirus and ICP6 encoded by human herpes simplex virus 1 (HSV-1), are also capable of forming hetero-amyloids with RIP3 through a similar RHIM–RHIM interaction. However, they block the self-assembly of RIP3 into homo-fibrils, thereby hijacking necroptosis signaling (Pham *et al.*, 2019; Baker *et al.*, 2020; Shanmugam *et al.*, 2021).

Purified RHIM proteins possess an intrinsic capability to spontaneously form fibrils in vitro. The question of how spontaneous fibril formation is prevented in living organisms has been unanswered for an extended period. Recently, our research has identified HSPA8 as an amyloidase that specifically targets a hydrophobic hexapeptide motif (N(X1)ϕ(X3)) of RHIM proteins. The HSPA8 protein is a member of the Hsp70 family, which measures 70 kilodaltons. Additionally, it is referred to as Hsc70, and it is continuously and significantly expressed in the cytoplasm. By constitutively binding to RHIM proteins, HSPA8 inhibits their fibrillation and disassembles preformed RHIM fibrils; thus, in vivo, it effectively impedes the spontaneous initiation of necroptosis (Wu *et al.*, 2023).

Despite the critical role of HSPA8 in necroptosis, the therapeutic potential of inhibiting HSPA8 to enhance tumor necroptosis remains unknown. The ATP-binding pocket in the nucleotide binding domain (NBD) and the peptide binding cavity in the substrate binding domain (SBD) are two potential inhibitor binding sites of HSPA8. The chemical VER-155008 (VER), an ATP-competitive inhibitor binds to NBD of HSPA8, preventing allosteric regulation of HSPA8 (Williamson *et al.*, 2009; Schlecht *et al.*, 2013). The HSP70 inhibitor PES (2-phenylethynesulfonamide, also known as pifithrin-μ) was found to interact with SBD of HSPA8 (Leu *et al.*, 2011; Schlecht *et al.*, 2013), inhibiting its protein-folding activity (Yang *et al.*, 2021). Therefore, exploring combinations with other chemotherapeutic agents is necessary to achieve a more potent effect.

In this study, we demonstrate that chemical inhibition of HSPA8 by VER or PES markedly enhances the necroptosis of cancer cells. Mechanistically, pharmacological inhibition of HSPA8 impairs its ability to recognize and interact with RHIM proteins, including RIP3, as well as its capacity to disassemble RHIM amyloids. Notably, inhibiting HSPA8 alone has been reported to have limited efficacy in compromising cancer cell death (Schlecht *et al.*, 2013). Here we found the combination of HSPA8 inhibitors with microtubule-targeting agents (MTAs), such as vincristine (VCR) and paclitaxel (PTX), significantly potentiates tumor regression in vivo. These findings highlight the therapeutic promise of targeting HSPA8 and suggest a novel chemo-combination strategy involving MTA drugs and HSPA8 inhibitors for a significantly more effective approach to cancer treatment.

## RESULTS

### Pharmacological inhibition targeting either the NBD or the SBD of HSPA8 promotes cancer cell necroptosis

VER and PES specifically target the NBD and SBDs of HSPA8, respectively. Utilizing L929 cells, an immortalized mouse fibroblast cell line that exhibits sensitivity to necroptosis, we investigated the effects of VER and PES on necroptosis induction. At concentrations lower than 3 μM, VER and PES did not exhibit noteworthy cytotoxic effects on L929 cells. Prior to the induction of necroptosis using TNF-α and z-VAD, L929 cells were exposed to different concentrations (1.5 μM or 3 μM) of HSPA8 inhibitors, VER and PES, for a duration of 2 h. Nec-1s, a particular inhibitor of necroptosis, acted via inhibiting the RIP1 kinase (Degterev *et al.*, 2005; Teng *et al.*, 2005; Degterev *et al.*, 2008; Takahashi *et al.*, 2012). The vehicle control consisted of an equal volume of DMSO (Figure 1, A and B). This finding is further validated in an additional cancer cell line, specifically the RIP3-expressing HeLa cells (Figure 1, C and D). Our results demonstrated that both VER and PES potentiated TNF-induced necroptosis in a dose-dependent manner (Figure 1). Overall, our data demonstrate that pharmacological inhibition targeting either the NBD or the SBD of HSPA8 promotes necroptosis.

### HSPA8 inhibitors boost MTA-induced cancer cell necroptosis even with modest MTA effects alone

MTAs bind to microtubules and modulate their dynamic properties. These agents have been widely used as anticancer chemotherapy drugs, including VCR and PTX (Brown *et al.*, 2023). MTA-induced microtubule disruption often leads to cell cycle arrest in rapidly dividing cells. Our previous study demonstrated that treatment with MTA family drugs in both dividing and nondividing cancer cells results in the accumulation of membrane TNF (memTNF) through the JNK/c-Jun axis, triggering adjacent cell death via TNFR signaling (Zhang *et al.*, 2019).

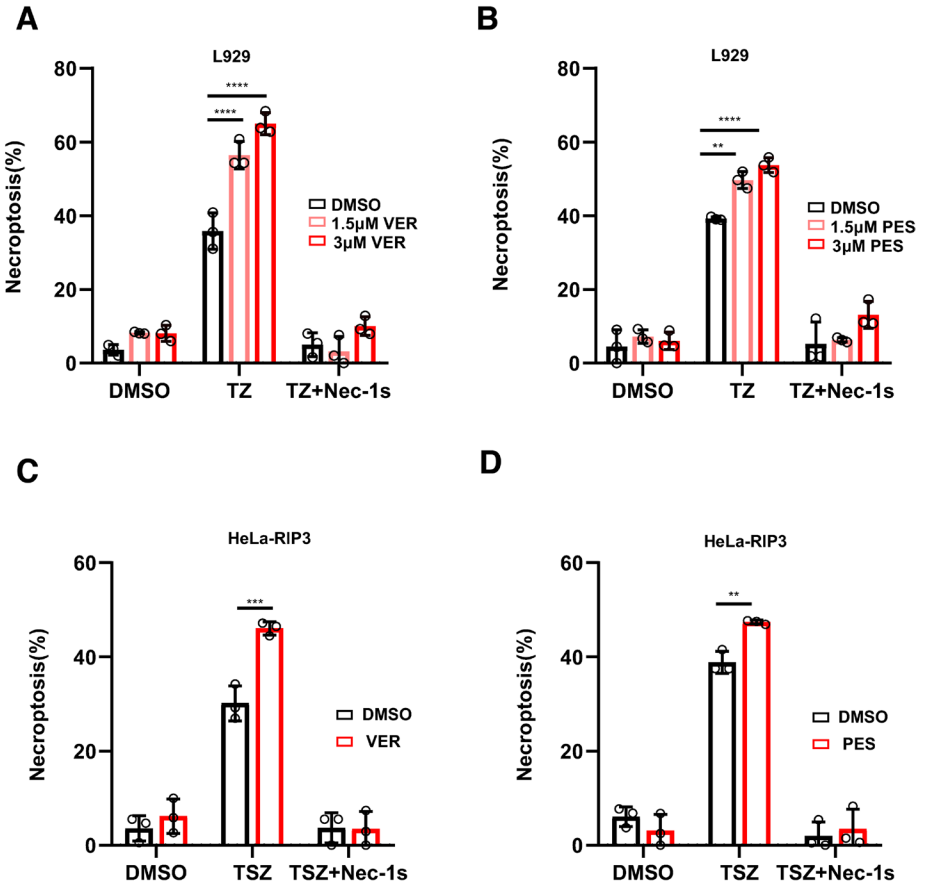


FIGURE 1: Pharmacological inhibition targeting either the NBD or the SBD of HSPA8 promotes necroptosis. (A and B) Impact of VER/PES on TNF-induced necroptosis in L929 cells. Cells were pretreated with varying concentrations of the HSPA8 inhibitor VER/PES for 2 h. Subsequently, necroptosis was triggered by treating the cells with TNF-α and Z-VAD-FMK (T/Z) for 3 h, with or without the addition of the necroptosis inhibitor Nec-1s at a concentration of 10 μM. The same-volume DMSO was used as the vehicle control. Cell viability was determined by measuring intracellular ATP levels. (C and D) Impact of VER/PES on TNF-induced necroptosis in Flag-RIP3–expressing HeLa cells. Cells were pretreated with the HSPA8 inhibitor VER (3 μM) or PES (5 μM) for 2 h. Following that, necroptosis was induced by exposing the cells to TNF-α, Smac, and z-VAD-FMK (T/S/Z) for 8 h, either with or without the inclusion of the necroptosis inhibitor Nec-1s at a dosage of 10 μM. Cell viability was determined by measuring intracellular ATP levels. Necroptosis inducer T/Z: T, TNFα (20 ng/mL); Z, z-VAD (20 μM). A, C for VER; B, D for PES. Data are presented as mean ± SD (s.d.) of biological triplicates. Groups were compared using an unpaired two-sided Student's *t* test. **, $p < 0.01$; ****, $p < 0.0001$.

Here, we found that treatment with the HSPA8 inhibitor PES significantly enhances MTA (VCR and PTX)-induced cell death, and this effect can be blocked by the necroptosis inhibitor Nec-1s (Figure 2, A and B). Furthermore, this enhancement is dose dependent, with higher concentrations of VCR or PTX resulting in more pronounced necroptosis. Through immunoblotting, we confirmed the necroptosis markers p-RIP3 and p-MLKL, thereby verifying that PES promotes MTA-induced necroptosis (Figure 2C). Our findings suggest that HSPA8 inhibitors can potentiate MTA-induced necroptosis in cancer cells, even when the effects of MTAs alone are comparably modest.

## HSPA8 inhibitors block HSPA8-mediated RIP3 fibril disassembly

Similar to other hsp70 proteins, the SBD of HSPA8 interacts directly with its substrate, the RHIM proteins. Given that PES specifically targets the SBD of HSPA8, we aimed to investigate whether PES disrupts the interaction between HSPA8 and the RHIM domain. To this end, we coexpressed HSPA8 and the RIP3-RHIM domain in 293T cells and assayed their interactions in the presence or absence of PES treatment. Our results revealed that PES treatment disrupts the recognition of the RIP3-RHIM domain by HSPA8 (Figure 3A).

The amyloidase activity of HSPA8 relies on its ATP hydrolysis to generate the necessary energy, which enables HSPA8 to disassemble RHIM fibrils and thus suppress necroptosis (Wu *et al.*, 2023). VER is a competitive inhibitor of HSPA8's ATPase activity, achieving this by competing with ATP and ADP for binding to the adenine pocket within the NBD of HSPA8 (Williamson *et al.*, 2009; Schlecht *et al.*, 2013). Subsequently, we conducted an in vitro RHIM amyloid disassembly assay to directly assess the impact of PES or VER on the amyloidase activity of HSPA8. In this assay, preformed RIP3 fibrils were incubated with HSPA8. After centrifugation, the fibrils were pelleted, while the disassembled RIP3 proteins remained in the supernatant fraction. Our findings revealed that the amount of RIP3 monomers dissolved in the supernatant decreased in the presence of both VER and PES (Figure 3B). Specifically, Line #1 serves as a negative control where RIP3 fibrils were not incubated with either HSPA8 or HSPA8 inhibitors. Consequently, most of the RIP3 fibrils stayed in the P fraction, as evident in lane #5. For the positive control, shown in lanes #2 and #6, RIP3 fibrils were incubated with HSPA8. This led to the disassembly of RIP3 fibrils, resulting in a decrease in the P fraction (lane #6) and an increase in the supernatant (S fraction, lane #2).

When the HSPA8-mediated disassembly assay was performed in the presence of HSPA8 inhibitors VER or PES, RIP3 fibrils failed to disassemble due to the inhibition of HSPA8. This was reflected in no increase in the S fraction (lanes #3, #4) and no decrease in the P fraction (lanes #7, #8).

In addition, we analyzed the disassembled status of RIP3 using native gel electrophoresis (Figure 3C). After incubation with HSPA8, RIP3 fibrils were disassembled into oligomers and monomers, visible as distinct upper bands on the gel (lane #2). However, the disassembly process was inhibited in the presence of an HSPA8 inhibitor, as evidenced by the absence of these bands (lane #3). Together, these results demonstrate that both VER and PES effectively inhibit the RHIM amyloid disaggregating activity of HSPA8.

## HSPA8 inhibitors overcome MTA chemoresistance to enhance tumor regression via necroptosis

MTAs have long reigned as the most successful chemotherapeutics on the market, but their clinical effectiveness is limited by side effects, including high systemic toxicity and the emergence of

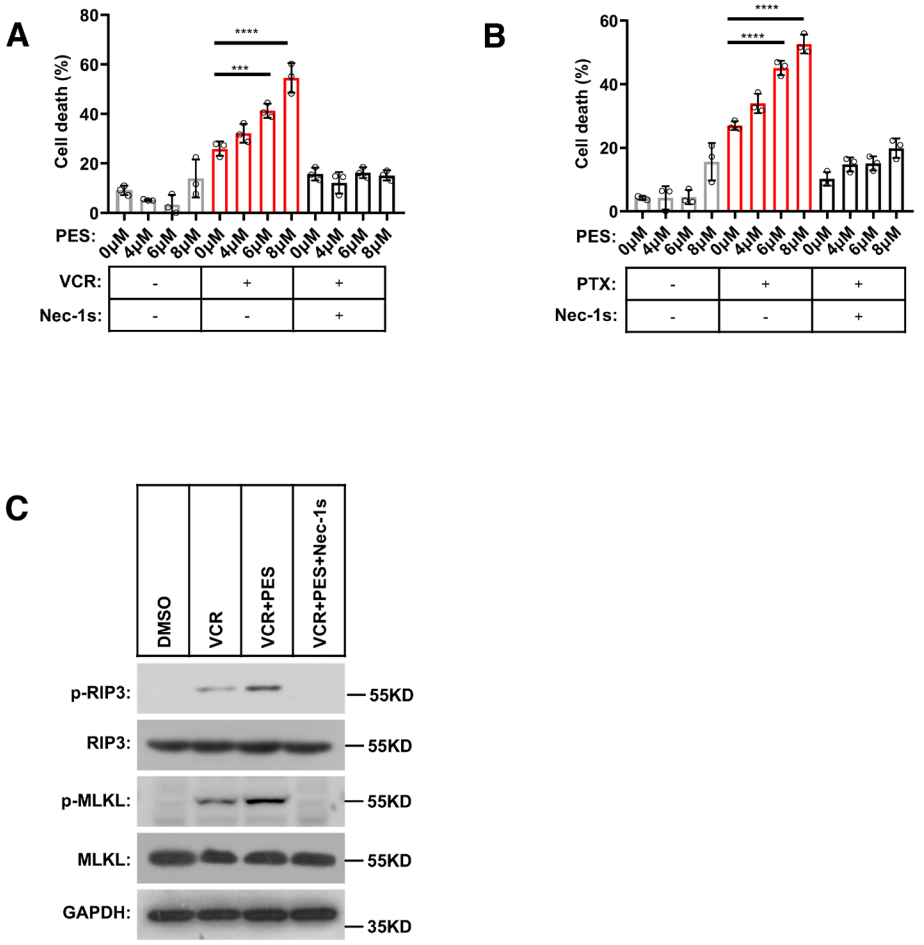


FIGURE 2: HSPA8 inhibitor boost MTA drug-induced necroptosis. (A and B) Effect of HSPA8 Inhibitor on MTA-induced necroptosis in L929 Cells. Cells were pretreated with various concentrations of the HSPA8 inhibitor PES for 2 h. Subsequently, necroptosis was triggered by treating the cells with VCR and PTX (VCR/PTX) for 24 h. The experiments were conducted with or without the addition of the necroptosis inhibitor Nec-1s at a concentration of 10 μM. c L929 cells were treated with the HSPA8 inhibitor PES (5 μM). Necroptosis was triggered by treating the cells VCR (150 nM) for 24 h. The experiments were conducted with or without the addition of the necroptosis inhibitor Nec-1s at a concentration of 10 μM. The necroptosis molecular markers (p-RIP3 and p-MLKL) were analyzed with the indicated antibodies by immunoblotting. Cell viability was determined by measuring intracellular ATP levels. Necroptosis inducer: VCR, vincristine (150 nM); PTX, paclitaxel (400 nM). A for VCR; B for PTX. Data are presented as mean ± SD (s.d.) of biological triplicates. Groups were compared using an unpaired two-sided Student's *t* test (as shown in A and B). ***, $p$ <0.005; ****, $p$ <0.0001.

resistance. To mitigate these limitations and enhance treatment efficacy, combining MTAs with other anticancer agents has emerged as a promising strategy (Wordeman and Vicente, 2021).

We hypothesized that the integration of HSPA8 inhibitors with necroptosis-inducing chemotherapeutic agents could potentially revolutionize cancer chemotherapy. Previous studies have demonstrated that MTAs can induce RIP3-MLKL–dependent necroptosis, leading to tumor shrinkage in L929 allografts (Zhang *et al.*, 2019). However, when using low concentrations of MTAs (0.5 mg/kg), L929-fibrosarcoma tumors showed minimal shrinkage (Figure 4D). Conversely, increasing the MTA concentration to a tumor-responsive dose (2 mg/kg) led to significant drug toxicity, ultimately resulting in mouse mortality (Figure 4B and C). This paradox highlights the inherent tension between efficacy and toxicity in most chemotherapeutics for patients. Notably, when combined with MTAs, HSPA8 inhibitors synergistically shrunk L929-fibrosarcoma tumors at concentrations where neither agent alone was effective (Figure 4D). Impressively, the mice remained vital and survived multiple injections, with constant tumor shrinkage, which could be blocked by the necroptosis inhibitor Nec-1s (Figure 4D).

## DISCUSSION

In this study, we demonstrated that HSPA8 inhibitors promote MTA-induced and TNF-induced necroptosis by suppressing HSPA8 amyloidase activity. Crucially, in vivo experiments revealed that combining HSPA8 inhibitors with MTAs effectively reduced the antitumor dosing requirement of MTAs, thereby minimizing their associated side effects. This finding suggests that HSPA8 inhibitors hold promising potential as anticancer agents especially for the necroptosis-sensitive cancers.

In practical clinical settings, MTAs typically require high concentrations to achieve optimal tumor cell killing. However, high doses of these chemotherapeutic agents inevitably result in toxicity to normal cells, manifesting as toxicities such as myelosuppression, gastrointestinal tract damage, and hair loss (Dominguez-Brauer *et al.*, 2015). Our findings indicate that inhibiting HSPA8 can enhance the tumoricidal activity of MTAs. By doing so, we were able to decrease the concentration of MTAs required to achieve therapeutic efficacy in a mouse fibrosarcoma model, thus avoiding their toxic side effects. Nevertheless, the impact of this combined therapy on patients with cancer remains to be fully elucidated.

VER and PES are small-molecule inhibitors that primarily target HSPA8. However, recent studies have identified additional targets for these inhibitors. Specifically, it has been reported that VER and PES interact with heat-inducible Hsp70 (HSPA1). This protein is marginally expressed in nontransformed cells but significantly overexpressed in tumor cells. Notably, silencing HSPA1 is cytotoxic to tumor cells but not to normal cells (Balaburski *et al.*, 2013; Schlecht *et al.*, 2013; Yang *et al.*, 2021). Nonetheless, based on our previous findings, HSPA1 does not play a role in suppressing necroptosis (Wu *et al.*, 2023). Considering this, targeting HSPA8 with VER/PES appears to be a promising anticancer clinical application, particularly for necroptosis-sensitive cancers that express RIP3. To fully realize the potential of these inhibitors, it is important to separate their targeting capabilities for HSPA1 and HSPA8, as they may have different applications in various cancer scenarios. For instance, HSPA1 inhibitors could be effective in RIP3-low cancers, while HSPA8 inhibitors may be more suitable for RIP3-high cancers. Moving forward, the design and screening of specific inhibitors that exclusively target each HSP70 member represents a significant area of future research. This approach could pave the way for more targeted and effective cancer therapies.

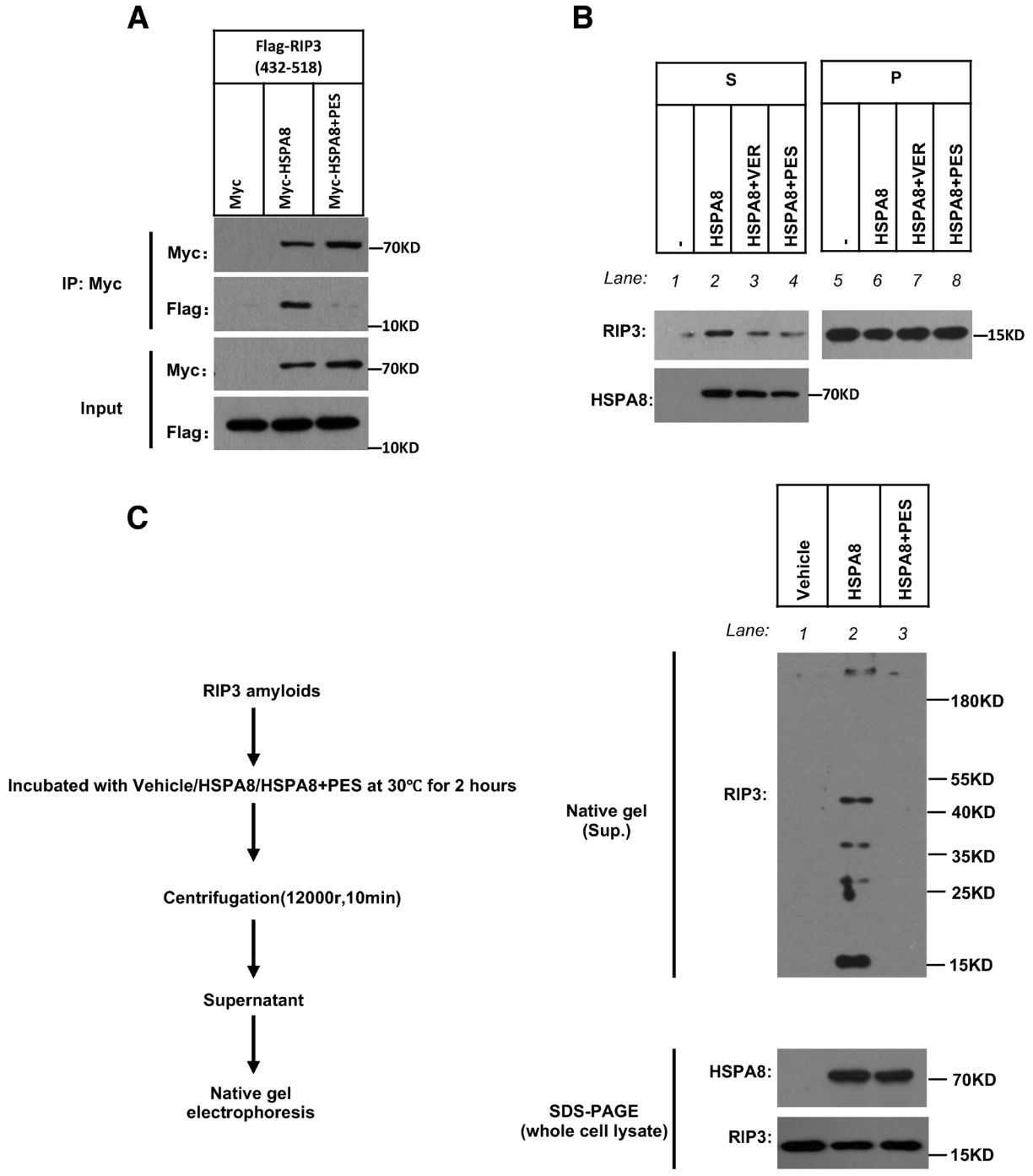


FIGURE 3: HSPA8 inhibitors block HSPA8-mediated RIP3 fibril disassembly. (A) Assessment of the impact of PES treatment on the interaction between HSPA8 and the RIP3-RHIM domain. Flag-tagged truncated RIP3 (amino acids 432-518) and Myc-tagged HSPA8 cDNAs were co-transfected into 293FT cells. Subsequently, the cells were treated with PES at a concentration of 3 mM. Following a 24-h transfection period, whole-cell lysates were prepared and immunoprecipitated using anti-Myc beads. The immunoprecipitates were then immunoblotted with the indicated antibodies to detect the interaction between HSPA8 and the RIP3-RHIM domain. (B) Test the inhibition of HSPA8-mediated disassembly of RIP3 amyloids by VER and PES. RIP3 monomer proteins were incubated at 37°C for 48 h to induce the formation of RIP3 amyloids. Subsequently, preformed RIP3 amyloids (5 μM) were incubated with HSPA8 (5 μM) in the presence or absence of VER or PES at 30°C for 120 min. Following incubation, the soluble RIP3 proteins and insoluble fibrils were separated by centrifugation at 12,000 × g for 10 min. The separated fractions were then analyzed by immunoblotting using anti-RIP3 antibodies. Left: Assay design for analyzing disassembled RIP3 through centrifugation. RIP3 fibrils were disassembled by incubating them with vehicle, HSPA8, or HSPA8+PES for 2 h at 30°C. Following the disassembly reaction, the RIP3 fragments in the supernatant were separated via centrifugation and run on a native gel (protein samples and gel processed without β-mercaptoethanol and SDS). Subsequently, immunoblotting was performed using the indicated antibodies (as shown in the right panels). All results are reported from one representative experiment from at least three independent repeats.

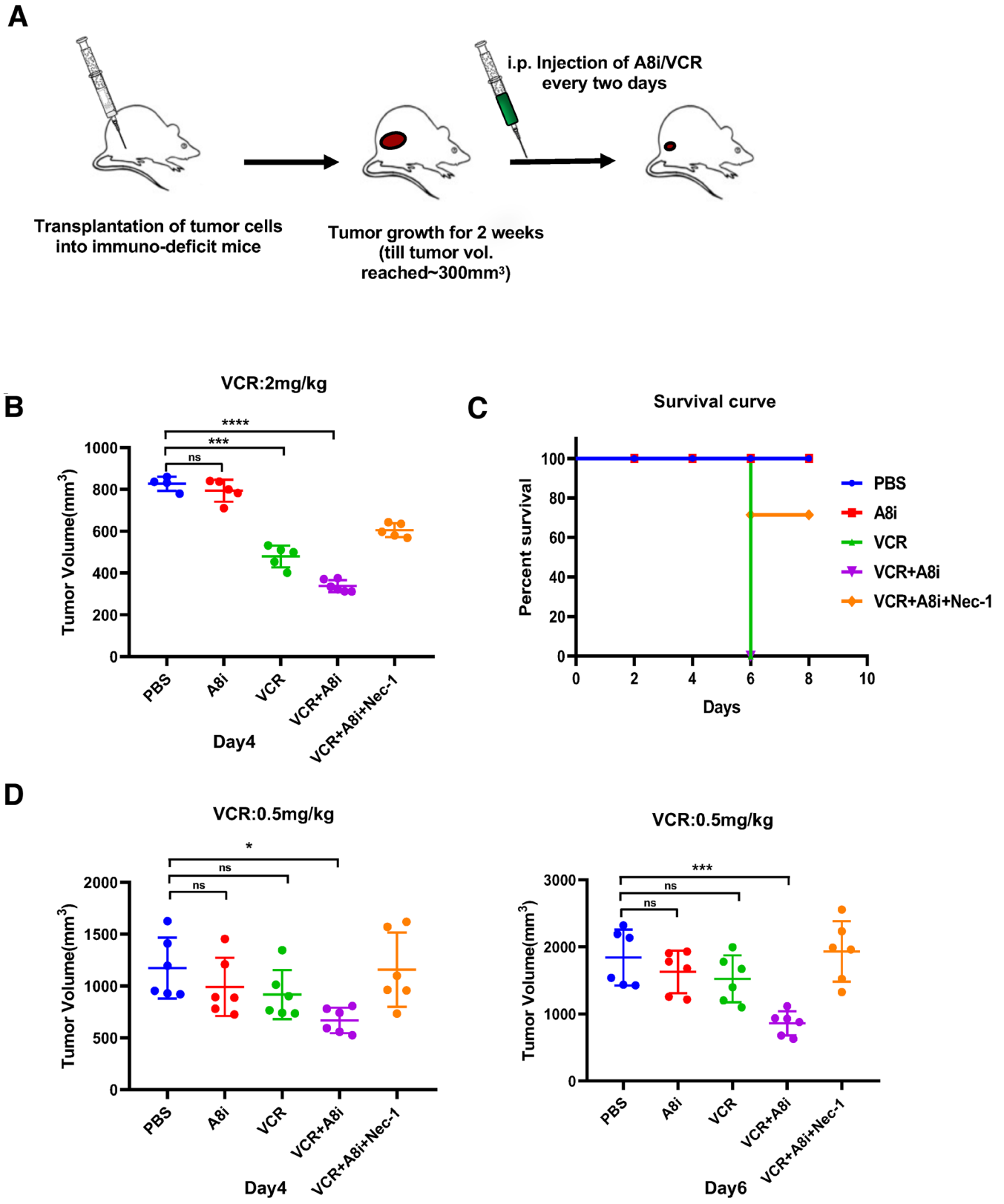


FIGURE 4: HSPA8 inhibitors promote MTA-induced tumor regression through enhancing necroptosis. (A) Schematic experimental design for HSPA8 inhibitor administration on tumor-bearing mice. Details are described in the *Materials and Methods*. (B) Impact of HSPA8 inhibitor on tumor shrinkage induced by high-dose MTA drugs. An allograft model using mouse L929 fibrosarcoma was established as outlined in the *Materials and Methods* section. Athymic nude mice bearing tumors approximately 300 $mm^3$ in size were randomly assigned to five different groups. Mice in each group were intraperitoneally (i.p.) injected with the specified compound combinations every 2 days. VCR: 2 mg/kg; PES: 12 mg/kg; Nec-1s: 5 mg/kg. The tumor volumes were measured on day 4. $n \geq 4$ for each group. $p$ values were determined

Importantly, PES has been found to promote cell cycle arrest by inhibiting the APC/C, thereby inducing G2/M arrest (Budina-Kolomets *et al.*, 2014). Therefore, it is essential to consider ways of decreasing cytotoxicity toward normal cells while enhancing the inhibitor's efficacy.

HSPA8, also known as Hsc70, is a member of the extensive HSP70 family and exhibits high expression levels in numerous cancer cells (Stricher *et al.*, 2014). Given its ubiquitous overexpression in most malignancies, HSPA8 has emerged as a potential alternative target for cancer therapy (Ying *et al.*, 2022). Theoretically, targeting HSPA8 with small-molecule inhibitors appears to be a promising approach for treating both cancer and autoimmune diseases. However, previous studies have encountered significant challenges due to the toxicity of HSPA8 inhibitors toward normal tissues (Mi *et al.*, 2021).

Our findings reveal that the use of lower concentrations of HSPA8 inhibitors that synergistically enhance the effects of MTAs at nontoxic concentrations appears to be a promising avenue for clinical exploration. This strategy could potentially lead to the development of more effective and safer cancer therapeutics. Future studies are needed to explore the efficacy and safety of combining HSPA8 inhibitors with MTAs in patients with cancer, to evaluate their therapeutic potential in clinical settings.

The necroptosis-inhibition function of HSPA8 is achieved by interfering with the formation of RHIM-amyloid structures (Wu *et al.*, 2023). RHIM proteins assemble into supramolecular structures through inter-RHIM interactions, playing a crucial role in the necroptosis signaling pathway, while also exhibiting other functions unrelated to cell death. It is well established that overexpression of RHIM proteins can activate NF-κB signaling in cells, and this activation can be suppressed through mutations in the RHIM domain that disrupt protein–protein interactions (Meylan *et al.*, 2004; Kaiser *et al.*, 2008). In the context of RNA virus infection in MLKL knockout cells, RIP1 binds with RIP3 and further recruits DRP1, forming the RIP1–RIP3–DRP1 complex. This complex activates the NLRP3 inflammasome, promoting an antiviral immune response (Wang *et al.*, 2014). However, the specific role of HSPA8 in these RHIM-mediated signaling pathways remains elusive. Given the potential of HSPA8 inhibitors to modulate NF-κB and NLRP3 inflammasome signaling in the tumor microenvironment, further exploration of their application in immunity is warranted. This could lead to the development of novel therapeutic strategies that harness the immunomodulatory properties of HSPA8 inhibitors to enhance antitumor immune responses.

In this investigation, we found that HSPA8 inhibitors increase tumor death by promoting necroptosis in cancer cells expressing RIP3. Nevertheless, the presence of RIP3 is lacking in certain types of malignancies, primarily due to chromosomal methylation and the control exerted by oncogenes like AXL and BRAF (Koo *et al.*, 2015; Green *et al.*, 2018). While RIP3 expression has been identified and documented in specific cancer types, including breast cancer, colorectal cancer, melanoma, and pancreatic cancer (Gong *et al.*, 2019). Therefore, the presence of RIP3 could be considered as a biomarker for using HSPA8 inhibitor to eliminate cancer, serving as a signal for therapeutic guidance. HSPA8 inhibitors may offer enhanced therapeutic benefits in tumors that express RIPK3.

## MATERIALS AND METHODS

### Cell culture

The L929 and 293FT cells were cultivated in DMEM, which was enriched with 10% FBS and 100 units/ml penicillin/streptomycin. All cells were maintained at a temperature of 37°C in a humidified incubator containing 5% $CO_2$. Additionally, all cell lines underwent rigorous testing to confirm their *Mycoplasma*-negative status using the standard PCR method.

### Plasmids

For transient expression in 293FT cells, Myc-hHSPA8 and Flag-$RIP3_{(432\text{-}518)}$ were cloned into pLIBIN plasmid. The hHSPA8, and $hRIP3_{(388\text{-}518)}$ constructs were subcloned into the pE-SUMO vector with a 6 × His-Sumo tag. All proteins were expressed in *Escherichia coli* (*E. coli*) BL21 (DE3) and were purified by Ni-affinity and gel filtration chromatography.

### Antibodies and reagents

For immunoblotting, antibodies were sourced from Sigma-Aldrich, including anti-Flag-HRP (catalog no.: A8592) and anti-Myc-HRP (catalog no.: 16-213). Additionally, anti-HSPA8 antibodies were obtained from ABclonal (catalog no.: A10898). The anti-human RIP3 antibodies were specifically purified in our own laboratory.

The recombinant mouse TNF used in our experiments was purified within our laboratory facilities and the endotoxins or lipopolysaccharides was removed by Endotoxin Removal Kit (catalog no.: Beyotime, catalog no. C0268S). PTX (catalog no.: #S1150) and VCR (catalog no.: #S1241) were purchased from Selleck Chemicals. Other inhibitors and reagents, including z-VAD-FMK (catalog no.: HY-16658B), VER-155008 (catalog no.: HY-10941), and Pifithrin-μ (catalog no.: HY-10940), were acquired from MedChemExpress.

For protein pull-down experiments, Myc beads (catalog no.: #E6654) were purchased from Sigma-Aldrich. Nec-1 (catalog no.: #N9037) was also obtained from Sigma, while Nec-1s (catalog no.: #2263) was purchased from BioVision.

All reagents were stored and handled according to the manufacturer's instructions to ensure optimal performance in our experiments.

### TNF-induced cell death assay

L929 cells were seeded into a 96-well plate at a density of 8000 cells per well and incubated for 12 h to facilitate their adherence and readiness for subsequent treatments. Prior to TNF-α stimulation, the cells were pretreated with various concentrations of the HSPA8 inhibitor PES or VER for 2 h. Subsequently, the cells were exposed to TNF-α (20 ng/mL) in combination with z-VAD (20 μM) to induce

by the two-way ANOVA test; ns: not significant; ***, $p < 0.001$. ****, $p < 0.0001$. (C) Kaplan–Meier survival curve of the tumor-bearing mice after three injections of HSPA8 inhibitor PES with high dose VCR (2 mg/kg). $n = 6$ for each group. (D) Impact of HSPA8 inhibitor on tumor shrinkage induced by low-dose MTA drugs. An allograft model using mouse L929 fibrosarcoma was established as outlined in the Methods section. Athymic nude mice bearing tumors approximately 300 $mm^3$ in size were randomly assigned to five different groups. Mice in each group were intraperitoneally (i.p.) injected with the specified compound combinations every 2 days. VCR: 0.5 mg/kg; PES: 12 mg/kg; Nec-1s: 5 mg/kg. The tumor volumes were measured on day 4 and on day 6. $n = 6$ for each group. $p$ values were determined by the two-way ANOVA test; ns: not significant; *, $p < 0.05$; **, $p < 0.01$; ***, $p < 0.001$. All experiments were repeated independently for three times.

necroptosis. To investigate the involvement of necroptosis, some cells were also treated with Nec-1 (10 μM) in the presence or absence of TNF-α and Z-VAD. The cells were maintained under these conditions for 3 h to assess the effects of the various treatments on cell death.

### MTA-induced cell death assay

L929 cells were seeded into a 96-well plate at a density of 5000 cells per well and incubated for 12 h to ensure their adherence and readiness for subsequent treatments. Prior to MTA exposure, the cells were pretreated with various concentrations of the HSPA8 inhibitor PES for 2 h. Subsequently, the cells were treated with either 150 nM VCR or 400 nM PTX in the presence or absence of 10 μM Nec-1. The cells were maintained under these conditions for an additional 24 h to assess the effects of the MTA agents and Nec-1 on cell death.

### ATP assay

Cell viabilities were determined using the CellTiter-Glo Luminescent Cell Viability Assay Kit (Promega), following the manufacturer's instructions precisely. This assay quantifies the amount of ATP present in the cells, which is a direct indicator of cell viability. To specifically assess necroptosis, the cell viability measured after treatment was subtracted from the initial total cell viability.

### Co-immunoprecipitation assay

Cells were collected, gently washed with PBS, and resuspended in lysis buffer containing 1% Triton X-100, 150 mM NaCl, 20 mM Tris/HCl (pH 7.4), and 5% glycerol. To ensure the integrity of proteins and phosphorylation states, the lysis buffer was supplemented with proteinase inhibitor (Roche, catalog no. 16829800) and phosphatase inhibitor (Thermo Fisher Scientific, catalog no. A32957). The cell suspension was incubated on ice for 30 min to allow for efficient lysis and protein extraction.

Subsequently, the lysate was centrifuged at 13,000 × *g* at 4°C for 10 min to pellet insoluble debris and separate the cleared lysate. The protein concentration in the supernatant was accurately measured using the Bradford Protein Assay Kit (Sangon Biotech, catalog no. C503031) to ensure consistent loading for immunoprecipitation.

For immunoprecipitation, 2 mg of whole-cell lysate proteins from each sample were incubated with anti-Myc beads, which specifically bind to the Myc tag. This allowed for the isolation of Myc-tagged proteins and their interacting partners. Following incubation, the beads were washed to remove unbound proteins and then subjected to immunoblotting using the indicated antibodies.

### Recombinant protein purification

Plasmids were transformed into BL21 (DE3) competent *E. coli* cells. All proteins were purified as previously described (Wu *et al*., 2023). Protein expression was induced by adding 0.5 mM IPTG (AMRESCO, catalog no. 0487) at OD600 = 0.8. Cells were cultured at 16°C overnight. The harvested cells were lysed by lysis buffer containing 300 mM NaCl, 50 mM Tris-HCl pH 8.0, 200 μg/ml PMSF, and 0.2 mM β-mercaptoethanol) and sonicated. The supernatant was incubated with Ni-NTA agarose at 4°C for 1 h, respectively. The Ni-NTA agarose was subsequently washed and then eluted with 500 mM imidazole. The eluted protein was further purified by gel filtration chromatography using the Superdex 200 10/300 GL column (GE Healthcare) at 4°C in an ÄKTA FPLC system (GE Healthcare). Protein concentrations were determined by the Bradford assay using BSA as a standard.

### Amyloid disassembly assay

Fresh RIP3 amyloid fibrils were prepared by incubating the protein at 37°C for 48 h to promote fibril formation. Subsequently, preformed RIP3 fibrils (5 μM monomer concentration) were incubated at 30°C with HSPA8 (5 μM) for 120 min to assess the disassembly process. In reactions containing $MgCl_2$ (20 mM), ATP (5 mM), and DTT (2 mM) were also included to evaluate their potential effects on amyloid disassembly.

After the incubation period, the soluble disaggregation products were separated from insoluble fibrils by centrifugation at 12,000 × *g* for 10 min. The supernatant containing the soluble proteins was then collected and analyzed via western blot to detect the presence and identity of RIP3 protein fragments resulting from the disassembly process.

### L929 fibrosarcoma model

L929 fibrosarcoma cells ($1 \times 10^6$) were subcutaneously injected into the dorsal area of athymic nude mice to establish the tumor model. Tumor growth was monitored by regularly measuring the tumor volume, which was calculated using the formula: $a \times b^2 \times 0.5$ (where a represents the maximum diameter and *b* represents the minimum diameter). Once the tumor volume reached approximately 300 $mm^3$, the tumor-bearing mice were randomly divided into five treatment groups.

Each group received a specific treatment combination delivered through intraperitoneal injection every 2 days. The treatment groups comprised the following: vehicle control, PES (an HSPA8 inhibitor), VCR, PES+VCR, and PES+VCR+Nec-1s. This allowed for the evaluation of the therapeutic effects of the different treatment combinations on tumor growth.

Tumor size was carefully monitored and measured every 2 days to assess the response to treatment. This experimental setup enabled a comprehensive analysis of the antitumor activity of the various treatments in the L929 fibrosarcoma mouse model.

### Data availability

The original data used to support the findings of this study are available from the corresponding author upon request.

## ACKNOWLEDGMENTS

We thank Dr. Weiguo Zou for generously sharing reagents with us. We thank members of the Sun laboratory for their comments and suggestions. We thank the animal experiment technology Facility of SIBCB for helping with the mouse model construction. This work was supported by the National Key Research and Development Program of China (2023YFA0914903), CAS Youth Interdisciplinary Team, the National Natural Science Foundation of China (32050187), the innovative research team of high-level local universities in Shanghai (SHSMU-ZDCX20212000).

## REFERENCES

Ai Y, Meng Y, Yan B, Zhou Q, Wang X (2024). The biochemical pathways of apoptotic, necroptotic, pyroptotic, and ferroptotic cell death. Mol Cell 84, 170–179.

Baker M, Shanmugam N, Pham CLL, Strange M, Steain M, Sunde M (2020). RHIM-based protein: protein interactions in microbial defence against programmed cell death by necroptosis. Semin Cell Dev Biol 99, 86–95.

Baker MODG, Shanmugam N, Pham CLL, Ball SR, Sierecki E, Gambin Y, Steain M, Sunde M (2022). The RHIM of the immune adaptor protein TRIF forms hybrid amyloids with other necroptosis-associated proteins. Molecules 27, 3382.

Balaburski GM, Leu JI, Beeharry N, Hayik S, Andrake MD, Zhang G, Herlyn M, Villanueva J, Dunbrack, Jr. RL, Yen T, *et al.* (2013). A modified HSP70

inhibitor shows broad activity as an anticancer agent. Mol Cancer Res 11, 219–229.
Brown JS, Amend SR, Austin RH, Gatenby RA, Hammarlund EU, Pienta KJ (2023). Updating the definition of cancer. Mol Cancer Res 21, 1142–1147.
Budina-Kolomets A, Balaburski GM, Bondar A, Beeharry N, Yen T, Murphy ME (2014). Comparison of the activity of three different HSP70 inhibitors on apoptosis, cell cycle arrest, autophagy inhibition, and HSP90 inhibition. Cancer Biol Ther 15, 194–199.
Cai Z, Jitkaew S, Zhao J, Chiang HC, Choksi S, Liu J, Ward Y, Wu LG, Liu ZG (2014). Plasma membrane translocation of trimerized MLKL protein is required for TNF-induced necroptosis. Nat Cell Biol 16, 55–65.
Carneiro BA, El-Deiry WS (2020). Targeting apoptosis in cancer therapy. Nat Rev Clin Oncol 17, 395–417.
Chen X, Li W, Ren J, Huang D, He WT, Song Y, Yang C, Li W, Zheng X, Chen P, Han J (2014). Translocation of mixed lineage kinase domain-like protein to plasma membrane leads to necrotic cell death. Cell Res 24, 105–121.
Chen X, Zhu R, Zhong J, Ying Y, Wang W, Cao Y, Cai H, Li X, Shuai J, Han J (2022). Mosaic composition of RIP1-RIP3 signalling hub and its role in regulating cell death. Nat Cell Biol 24, 471–482.
Degterev A, Hitomi J, Germscheid M, Ch'en IL, Korkina O, Teng X, Abbott D, Cuny GD, Yuan C, Wagner G, *et al*. (2008). Identification of RIP1 kinase as a specific cellular target of necrostatins. Nat Chem Biol 4, 313–321.
Degterev A, Huang Z, Boyce M, Li Y, Jagtap P, Mizushima N, Cuny GD, Mitchison TJ, Moskowitz MA, Yuan J (2005). Chemical inhibitor of nonapoptotic cell death with therapeutic potential for ischemic brain injury. Nat Chem Biol 1, 112–119.
Dominguez-Brauer C, Thu KL, Mason JM, Blaser H, Bray MR, Mak TW (2015). Targeting mitosis in cancer: Emerging strategies. Mol Cell 60, 524–536.
Dondelinger Y, Declercq W, Montessuit S, Roelandt R, Goncalves A, Bruggeman I, Hulpiau P, Weber K, Sehon CA, Marquis RW, *et al*. (2014). MLKL compromises plasma membrane integrity by binding to phosphatidylinositol phosphates. Cell Rep 7, 971–981.
Dondelinger Y, Hulpiau P, Saeys Y, Bertrand MJM, Vandenabeele P (2016). An evolutionary perspective on the necroptotic pathway. Trends Cell Biol 26, 721–732.
Fanale D, Iovanna JL, Giordano A, Rolfo C, Russo A (2017). Cancer clonal evolution and intra-tumor heterogeneity. In: Liquid Biopsy in Cancer Patients, eds. A Russo, A Giordano, and C Rolfo, Cham, Switzerland: Humana Press, https://doi.org/10.1007/978-3-319-55661-1_3.
Gong Y, Fan Z, Luo G, Yang C, Huang Q, Fan K, Cheng H, Jin K, Ni Q, Yu X, Liu C (2019). The role of necroptosis in cancer biology and therapy. Mol Cancer 18, 100.
Green D, Najafov A, Zervantonakis IK, Mookhtiar AK, Greninger P, March RJ, Egan RK, Luu HS, Stover DG, Matulonis UA, *et al*. (2018). BRAF and AXL oncogenes drive RIPK3 expression loss in cancer. PLoS Biol 16, e2005756.
Grootjans S, Vanden Berghe T, Vandenabeele P (2017). Initiation and execution mechanisms of necroptosis: an overview. Cell Death Differ 24, 1184–1195.
He S, Liang Y, Shao F, Wang X (2011). Toll-like receptors activate programmed necrosis in macrophages through a receptor-interacting kinase-3-mediated pathway. Proc Natl Acad Sci USA 108, 20054–20059.
Hildebrand JM, Tanzer MC, Lucet IS, Young SN, Spall SK, Sharma P, Pierotti C, Garnier JM, Dobson RC, Webb AI, *et al*. (2014). Activation of the pseudokinase MLKL unleashes the four-helix bundle domain to induce membrane localization and necroptotic cell death. Proc Natl Acad Sci USA 111, 15072–15077.
Hu H, Wu X, Wu G, Nan N, Zhang J, Zhu X, Zhang Y, Shu Z, Liu J, Liu X, *et al*. (2021). RIP3-mediated necroptosis is regulated by inter-filament assembly of RIP homotypic interaction motif. Cell Death Differ 28, 251–266.
Kaiser WJ, Upton JW, Mocarski ES (2008). Receptor-interacting protein homotypic interaction motif-dependent control of NF-κB activation via the DNA-dependent activator of IFN regulatory factors. J Immunol 181, 6427–6434.
Koo G-B, Morgan MJ, Lee D-G, Kim W-J, Yoon J-H, Koo JS, Kim SI, Kim SJ, Son MK, Hong SS, *et al*. (2015). Methylation-dependent loss of RIP3 expression in cancer represses programmed necrosis in response to chemotherapeutics. Cell Res 25, 707–725.
Leu JIJ, Pimkina J, Pandey P, Murphy ME, George DL (2011). HSP70 inhibition by the small-molecule 2-phenylethynesulfonamide impairs protein clearance pathways in tumor cells. Mol Cancer Res 9, 936–947.
Li J, McQuade T, Siemer AB, Napetschnig J, Moriwaki K, Hsiao YS, Damko E, Moquin D, Walz T, McDermott A, *et al*. (2012). The RIP1/RIP3 necrosome forms a functional amyloid signaling complex required for programmed necrosis. Cell 150, 339–350.
Meier P, Legrand AJ, Adam D, Silke J (2024). Immunogenic cell death in cancer: targeting necroptosis to induce antitumour immunity. Nat Rev Cancer 24, 299–315.
Meylan E, Burns K, Hofmann K, Blancheteau V, Martinon F, Kelliher M, Tschopp J (2004). RIP1 is an essential mediator of Toll-like receptor 3–induced NF-κB activation. Nat Immunol 5, 503–507.
Mi J, Yang Y, Yao H, Huan Z, Xu C, Ren Z, Li W, Tang Y, Fu R, Ge X (2021). Inhibition of heat shock protein family A member 8 attenuates spinal cord ischemia–reperfusion injury via astrocyte NF-κB/NLRP3 inflammasome pathway. J Neuroinflammation 18, 170.
Mompeán M, Li W, Li J, Laage S, Siemer AB, Bozkurt G, Wu H, McDermott AE (2018). The structure of the necrosome RIPK1-RIPK3 core, a human hetero-amyloid signaling complex. Cell 173, 1244–1253.e1210.
Morgan MJ, Kim YS (2022). Roles of RIPK3 in necroptosis, cell signaling, and disease. Exp Mol Med 54, 1695–1704.
Pasparakis M, Vandenabeele P (2015). Necroptosis and its role in inflammation. Nature 517, 311–320.
Pham CL, Shanmugam N, Strange M, O'Carroll A, Brown JW, Sierecki E, Gambin Y, Steain M, Sunde M (2019). Viral M45 and necroptosis-associated proteins form heteromeric amyloid assemblies. EMBO Rep 20, e46518.
Schlecht R, Scholz SR, Dahmen H, Wegener A, Sirrenberg C, Musil D, Bomke J, Eggenweiler HM, Mayer MP, Bukau B (2013). Functional analysis of Hsp70 inhibitors. PLoS One 8, e78443.
Shanmugam N, Baker MODG, Sanz-Hernandez M, Sierecki E, Gambin Y, Steain M, Pham CLL, Sunde M (2021). Herpes simplex virus encoded ICP6 protein forms functional amyloid assemblies with necroptosis-associated host proteins. Biophys Chem 269, 106524.
Stricher F, Macri C, Ruff M, Muller S (2014). HSPA8/HSC70 chaperone protein. Autophagy 9, 1937–1954.
Sun L (2023). Amyloids as kinase signalling platforms. Nat Rev Mol Cell Biol 24, 85.
Sun L, Wang H, Wang Z, He S, Chen S, Liao D, Wang L, Yan J, Liu W, Lei X, Wang X (2012). Mixed lineage kinase domain-like protein mediates necrosis signaling downstream of RIP3 kinase. Cell 148, 213–227.
Sun L, Wang X (2014). A new kind of cell suicide: mechanisms and functions of programmed necrosis. Trends Biochem Sci 39, 587–593.
Takahashi N, Duprez L, Grootjans S, Cauwels A, Nerinckx W, DuHadaway JB, Goossens V, Roelandt R, Van Hauwermeiren F, Libert C, *et al*. (2012). Necrostatin-1 analogues: critical issues on the specificity, activity and in vivo use in experimental disease models. Cell Death Dis 3, e437.
Teng X, Degterev A, Jagtap P, Xing X, Choi S, Denu R, Yuan J, Cuny GD (2005). Structure-activity relationship study of novel necroptosis inhibitors. Bioorg Med Chem Lett 15, 5039–5044.
Tummers B, Green DR (2022). Mechanisms of TNF-independent RIPK3-mediated cell death. Biochem J 479, 2049–2062.
Upton JW, Kaiser WJ, Mocarski ES (2012). DAI/ZBP1/DLM-1 complexes with RIP3 to mediate virus-induced programmed necrosis that is targeted by murine cytomegalovirus vIRA. Cell Host Microbe 11, 290–297.
Vanden Berghe T, Hassannia B, Vandenabeele P (2016). An outline of necrosome triggers. Cell Mol Life Sci 73, 2137–2152.
Wang H, Sun L, Su L, Rizo J, Liu L, Wang LF, Wang FS, Wang X (2014). Mixed lineage kinase domain-like protein MLKL causes necrotic membrane disruption upon phosphorylation by RIP3. Mol Cell 54, 133–146.
Wang X, Jiang W, Yan Y, Gong T, Han J, Tian Z, Zhou R (2014). RNA viruses promote activation of the NLRP3 inflammasome through a RIP1-RIP3-DRP1 signaling pathway. Nat Immunol 15, 1126–1133.
Williamson DS, Borgognoni J, Clay A, Daniels Z, Dokurno P, Drysdale MJ, Foloppe N, Francis GL, Graham CJ, Howes R, *et al*. (2009). Novel adenosine-derived inhibitors of 70 kDa heat shock protein, discovered through structure-based design. J Med Chem 52, 1510–1513.
Wordeman L, Vicente JJ (2021). Microtubule targeting agents in disease: Classic drugs, novel roles. Cancers 13, 5650.
Wu E, He W, Wu C, Chen Z, Zhou S, Wu X, Hu Z, Jia K, Pan J, Wang L, *et al*. (2023). HSPA8 acts as an amyloidase to suppress necroptosis by inhibiting and reversing functional amyloid formation. Cell Res 33, 851–866.

Wu X, Ma Y, Zhao K, Zhang J, Sun Y, Li Y, Dong X, Hu H, Liu J, Wang J, *et al*. (2021). The structure of a minimum amyloid fibril core formed by necroptosis-mediating RHIM of human RIPK3. Proc Natl Acad Sci USA 118, e2022933118.

Wu XL, Hu H, Dong XQ, Zhang J, Wang J, Schwieters CD, Liu J, Wu GX, Li B, Lin JY, *et al*. (2021). The amyloid structure of mouse RIPK3 (receptor interacting protein kinase 3) in cell necroptosis. Nat Commun 12, 1627.

Wu XN, Yang ZH, Wang XK, Zhang Y, Wan H, Song Y, Chen X, Shao J, Han J (2014). Distinct roles of RIP1-RIP3 hetero- and RIP3-RIP3 homo-interaction in mediating necroptosis. Cell Death Differ 21, 1709–1720.

Yang J, Gong W, Wu S, Zhang H, Perrett S (2021). PES inhibits human-inducible Hsp70 by covalent targeting of cysteine residues in the substrate-binding domain. J Biol Chem 296, 100210.

Ying B, Xu W, Nie Y, Li Y, Bukhari I (2022). HSPA8 is a new biomarker of triple negative breast cancer related to prognosis and immune infiltration. Dis Markers 2022, 1–27.

Yuan J, Ofengeim D (2024). A guide to cell death pathways. Nat Rev Mol Cell Biol 25, 379–395.

Zhang J, Yang Y, Shen'ao S, He X, Cao X, Wu C, Hu H, Qin J, Wei G, Wang H, *et al*. (2019). Membrane-bound TNF mediates microtubule-targeting chemotherapeutics-induced cancer cytolysis via juxtacrine inter-cancer-cell death signaling. Cell Death Differ 27, 1569–1587.